

# Nonlinear Faraday Rotation and Superposition-State Detection in Cold Atoms

Adam Wojciechowski,<sup>1,2</sup> Eric Corsini,<sup>3,2</sup> Jerzy Zachorowski,<sup>1,2</sup> and Wojciech Gawlik<sup>1,2</sup>

<sup>1</sup>*Institute of Physics, Jagiellonian University, Reymonta 4, PL-30-059 Kraków, Poland*

<sup>2</sup>*Joint Krakow-Berkeley Atomic Physics and Photonics Laboratory, Reymonta 4, PL-30-059 Kraków, Poland*

<sup>3</sup>*Department of Physics, University of California, Berkeley, CA 94720-7300, USA*

(Dated: January 11, 2010)

We report on the first observation of nonlinear Faraday rotation with cold atoms at a temperature of  $\sim 100 \mu\text{K}$ . The observed nonlinear rotation of the light polarization plane is up to 0.1 rad over the 1 mm size atomic cloud in approximately 10 mG magnetic field. The nonlinearity of rotation results from long-lived coherence of ground-state Zeeman sublevels created by a near-resonant light. The method allows for creation, detection and control of atomic superposition states. It also allows applications for precision magnetometry with high spatial and temporal resolution.

PACS numbers: 33.57.+c, 42.50.Dv, 42.50.Gy, 32.80.Xx

The linear Faraday rotation (LFR) of the polarization plane of light propagating in the medium is a well known consequence of optical anisotropy caused by a longitudinal magnetic field. For thermal gases the Doppler effect broadens the range of the magnetic fields where the effect is visible and reduces the size of the maximum rotation relative to atoms at rest. The use of cold atoms with their Doppler width narrower than the natural linewidth distinguishes this situation from experiments at room temperature. The experiments on LFR with cold atoms were performed in a magneto-optical trap (MOT) [1–3], and in an optical dipole trap [4].

Application of strong, near-resonant laser light may result in the creation of coherent superpositions of Zeeman sublevels of an atomic ground state. Such superpositions (Zeeman coherences) are known to be responsible for a variety of coherent phenomena in light-matter interaction, like coherent population trapping [5], electromagnetically-induced transparency [6], nonlinear magneto-optical rotation or nonlinear Faraday rotation (NFR) [7] and their interplay [8]. Superposition states are also at the heart of quantum-state engineering (QSE). Most of QSE experiments require initial states of well defined atomic spin (or total angular momentum  $F$ ), usually prepared in a stretched state, which is realized by putting most of (ideally all) atomic population into a Zeeman sublevel with extreme value of magnetic quantum number  $m$  [9]. Below we report how superpositions of specific Zeeman sublevels, or Zeeman coherences belonging to a given  $F$  are created in cold ( $\sim 100 \mu\text{K}$ ) atomic samples and observed with high sensitivity using nonlinear Faraday rotation. In the experiment laser light both creates and detects the Zeeman coherences. The same detection technique can be applied to detect the presence of Zeeman coherences already introduced with other mechanisms. Furthermore, the time-dependent detection provides information on the temporal evolution of the superposition states.

The described experiment shows the potential of NFR with cold atoms for precision magnetometry with

prospective  $\mu\text{G}$  sensitivity, large dynamic range (zero-field to several G), and sub-mm spatial resolution in magnetic field mapping. Magnetic field sensing with cold atoms utilizing Larmor precession of alkali atoms in a magnetic field has been discussed in: MOT [10], Bose-Einstein condensate [11, 12] and an optical dipole trap [13]. Our measurements apply a different principle: rather than measuring Larmor frequency (single atom quantity), we measure rotation of a polarization plane (a cumulative effect over the whole sample), which may offer higher accuracy in very low magnetic fields. In our experiment the rotation is mainly caused by the nonlinear medium's birefringence resulting from the light-induced Zeeman coherences [14, 15], regarded as the diamagnetic effect. The rotation resulting from population imbalance (paramagnetic effect) was studied with cold atoms in recent experiments devoted to spin squeezing [16].

For resonant excitation, rotation angle  $\theta$  is a measure of circular birefringence,  $\theta \propto (n_+ - n_-)$ , where  $n_{\pm}$  are the refractive indices for  $\sigma^{\pm}$  polarized light and  $n_{\pm} - 1 \propto \mathcal{E}^{-1} \sum_{eg} \text{Re}(d_{eg} \rho_{eg})$  with  $\mathcal{E}$  being the light electric field amplitude,  $d_{eg}$  the dipole moment, and  $\rho_{eg}$  the density matrix element. The summation goes over all ground- and excited-state sublevels  $g$  and  $e$  linked by the allowed transitions, as shown in Fig. 1b. In the stationary regime,  $\rho_{eg}$  can be expressed as  $\rho_{eg} = \sum_{e'g'} (\Omega_{eg'} \rho_{g'g} - \rho_{ee'} \Omega_{e'g}) / (\delta_{eg} - i\Gamma/2)$ , where  $\delta_{\alpha\beta}$  and  $\Omega_{\alpha\beta}$  denote respectively the light detuning and Rabi frequency for the  $\alpha \leftrightarrow \beta$  transition, and  $\Gamma/2$  is the relaxation rate of the optical coherence. This relation indicates that optical coherences, and consequently also the refractive indices and rotation angle, depend on the density matrix elements  $\rho_{g'g}$  and  $\rho_{ee'}$  which represent populations of and coherences between Zeeman sublevels of the ground and excited states. For not-too-strong light, the excited-state coherences are negligible and all couplings shown in Fig. 1b form independent generic  $\Lambda$ -systems which involve coherences between ground-state sublevels with  $\Delta m = \pm 2$ .

The main difficulty in observation of NFR with cold

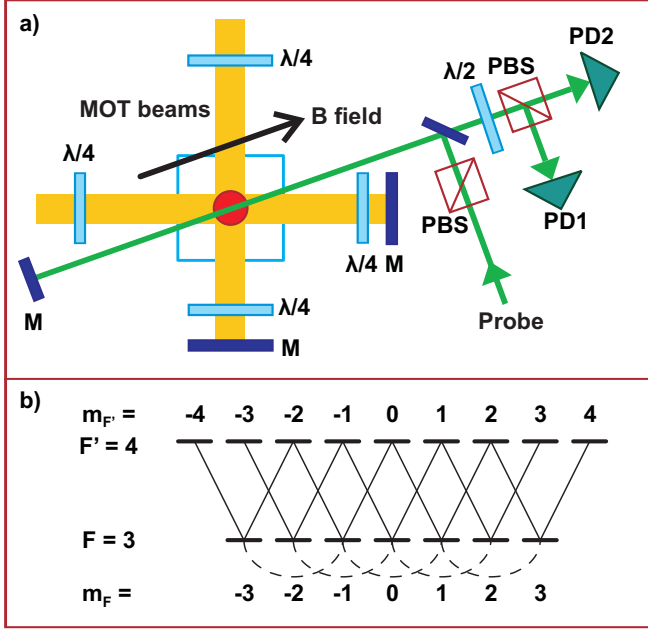


FIG. 1: (a) The setup of the experiment for the balanced polarimeter arrangement. M are mirrors, PBS polarizing beam splitters, PD photodetectors,  $\lambda/2$ ,  $\lambda/4$  waveplates. Direction of the magnetic field  $B$  necessary for the observation of the Faraday rotation is indicated. (For FS scheme the  $\lambda/2$  plate is removed and PD2 is not used). (b) Energy level-structure with the Zeeman-coherences established by a linearly-polarized light.

atoms is that at light intensity required for creation of the Zeeman coherence the laser beam may mechanically perturb the cold-atom sample. In our study this adverse effect is reduced by retroreflection of the light beam and careful optimization of the experimental conditions to minimize the light power.

The experiment (see the setup shown in Fig. 1a) was performed with about  $10^7$   $^{85}\text{Rb}$  atoms using a standard MOT. In addition to the trapping and repumping lasers we used a separate probe laser whose frequency was tuned around the  $F = 3 \rightarrow F' = 4$  hyperfine transition of the D2 line (780nm). Fig. 1b depicts the Zeeman structure of the  $F = 3$  and  $F' = 4$  states with the transitions induced by linearly polarized light (superposition of  $\sigma^\pm$  polarizations). A weak linearly polarized probe beam of several  $\mu\text{W}$  in power and 2 mm in diameter was sent through the atom cloud and then retroreflected to partially reduce light pressure effects. The probe-beam frequency 14 MHz below the line center proved to be optimal from the point of view of atomic loss which we attribute to extra Doppler-cooling mechanism by two counter-propagating beams. The double passage of light through the sample doubled the acquired Faraday rotation. The light polarization was measured in two arrangements: using balanced polarimeter (direct rotation angle measurement) and in a crossed polarizers or forward-scattering (FS)

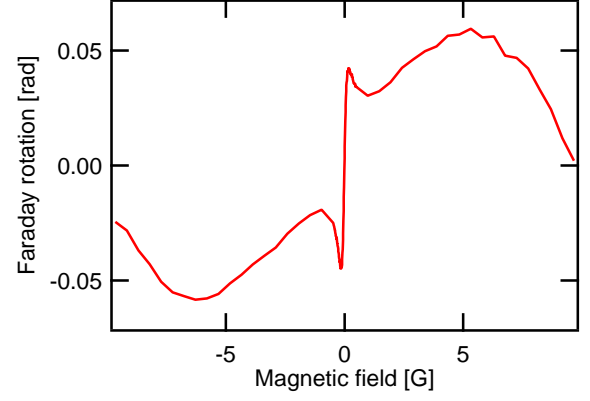


FIG. 2: Linear (wide) and nonlinear (narrow) Faraday rotation resonances centered at  $B = 0$ . NFR resonance is power broadened for a better visibility. The probe power is  $64 \mu\text{W}$ .

scheme which for resonant light is sensitive to the square of the rotation angle. For non-resonant case, circular dichroism contributes also to the observed signal.

In the experiment atoms were collected and cooled in the MOT. This phase was periodically interrupted for the measurement of optical rotation: the MOT lasers and the quadrupole magnetic field were switched off and a homogenous magnetic field  $B$  of a controlled value was applied along the probe beam. After 2 ms (required for complete decay of the eddy currents induced by turning off the quadrupole field) the probe beam was switched on and polarization rotation was recorded for the next 5 ms. Finally, the MOT fields were switched back for 50–200 ms and the atomic cloud was recaptured and cooled. This procedure allowed recording polarization rotation signals as a function of time for each value of the  $B$  field. The experiment was controlled by a PC, which also digitized, stored, and averaged (typically 20 times) the data.

Typical signals (rotation angle vs.  $B$ ) associated with linear and nonlinear Faraday effect have the form of dispersive resonances nested at  $B = 0$ , as shown in Fig. 2. The narrow feature is the nonlinear resonance (NFR); it appears when the probe beam is sufficiently intense. Hereinafter, we refer to this nonlinear resonance as the zero-field resonance. The width of the linear resonance amounts to several G and corresponds to the natural linewidth of the studied transition. It also depends on the detuning of the probe beam from resonance condition and initial Zeeman-sublevel populations, as has been shown in [2]. That situation is prominently different from the case of vapor cells, where LFR resonance is two orders of magnitude broader, because of the Doppler effect

In Fig. 3 we depict the evolution of the Faraday rotation signals with the increase of the light power. While the wide structure associated with the linear Faraday effect represent rotation angle independent on the light intensity, the central narrow feature clearly exhibits non-

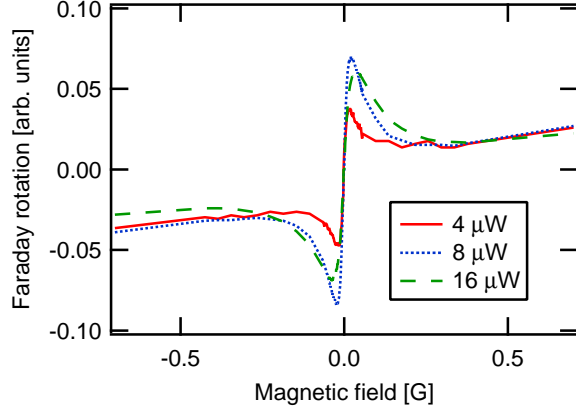


FIG. 3: Evolution of the Faraday rotation with increasing light intensity of the probe beam showing the nonlinear increase and power broadening of the central resonance.

linear behavior. The narrow part is due to the superpositions of the ground-state Zeeman sublevels which differ by  $|\Delta m| = 2$ , shown in Fig. 1b. These are thus the light-induced Zeeman coherences that are responsible for nonlinearity of the Faraday effect observed with appropriately strong light in very small magnetic fields. The narrow width reflects the long lifetime of the ground-state superpositions which is a necessary prerequisite for qubits and QSE applications. In case of atoms released from the MOT, the main mechanism of the resonance broadening is the escape time of atoms from the observation volume due to gravitation and their initial momenta. There is also light-induced expelling of atoms from the probed volume which can be seen in Fig. 3 as the drop of maximal rotation seen with 16  $\mu\text{W}$  relative to 8  $\mu\text{W}$ . Another major contribution comes from transverse magnetic fields, and can be understood as power broadening due to magnetically-driven transitions between degenerate Zeeman sublevels for the near-zero fields. Therefore, DC and low-frequency transverse magnetic field components have to be precisely compensated for the NFR observation. Other broadening mechanisms include gradient of the longitudinal magnetic field and power broadening due to the probing beam, which can be reduced by using appropriate intensity and detuning. The latter offers additional possibility of laser cooling for retroreflected, red detuned probe beam, as mentioned above.

Time evolution of Faraday rotation squared (FS-arrangement) is depicted in Fig. 4. The linear effect depends only on number of atoms and Zeeman population distribution and thus follows the temporal evolution of these quantities. The nonlinear effect results from light-atom interaction, i.e., optical pumping with linearly polarized light and thus requires some, light-intensity-dependent, time to build up. This effect can be seen in Fig. 5, where examples of such evolution for two different light intensities are presented. Unlike the linear contri-

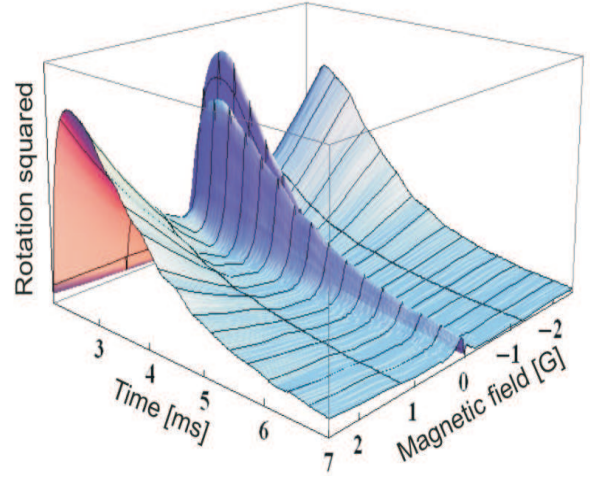


FIG. 4: Time evolution of linear (wide) and nonlinear (narrow) Faraday rotation resonances in FS-arrangement where the signal is proportional to magneto-optical rotation angle squared. Probe power is 18  $\mu\text{W}$ .

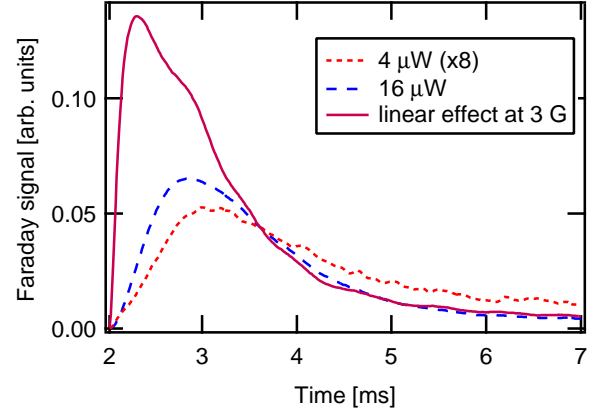


FIG. 5: Time dependence of the nonlinear Faraday rotation with a 45 mG magnetic field at two different probe beam powers (4  $\mu\text{W}$  - magnified 8 times and 16  $\mu\text{W}$ ) compared to the time dependence of the linear Faraday rotation at 3 G and 16  $\mu\text{W}$ .

bution, the onset of which is limited only by the detector time constant, the initial slopes of the nonlinear contributions indeed depend on the probe power. Both signals decay as atoms escape from the probed volume. The separation between the linear and nonlinear contributions corresponding to a given light power is done based on the magnetic field strength: at about 45 mG the LFR is negligible and NFR dominates the rotation, whereas the opposite is true for magnetic fields of 3 G and above.

Since the stationary ground-state coherences are destroyed when Larmor precession becomes faster than the coherence relaxation time, direct observation of the NFR signals is limited to a very narrow (some mG) range around  $B = 0$ . One possibility to observe NFR not

only around the zero magnetic field is to use modulation techniques. Two arrangements have been proposed using either frequency (FM NMOR [17]) or amplitude (AMOR [18]) modulation of light. In both arrangements strobed pumping creates the modulated Zeeman coherence and phase sensitive detection is used to extract the magneto-optical rotation amplitude. In addition to the zero-field resonance, two other resonances appear in the demodulated rotation signal when the modulation frequency  $\Omega_m$  meets  $\pm$  twice Larmor precession frequency in a given magnetic field. These high-field resonances result from the optical pumping synchronous with the Larmor precession. The factor of 2 appears because the two-fold symmetry of the optical anisotropy associated with  $|\Delta m| = 2$  coherences yields modulation at precisely twice the Larmor precession. The width of these resonances is determined by the coherence lifetime and, in case of long-lived ground states, can be as narrow as the zero field resonance.

In our experiment the AMOR technique was applied: the probe beam was periodically chopped using the acousto-optical modulators. Use of modulation frequencies up to  $\sim 10$  MHz allowed detection of resonances in magnetic fields as large as 9 G. This is an order of magnitude higher field compared to previous FM NMOR and AMOR work and demonstrates the method's potential for precision magnetometry in a wide range of fields. This range can be further extended by using electro-optical modulators up to the fields where the nonlinear Zeeman effect starts to affect the signals. Figure 6 shows NFR signal with two AMOR resonances at  $\pm 3$  G that are the evidence of driving  $|\Delta m| = 2$  coherences at non-zero magnetic fields.

In conclusion, we have demonstrated the nonlinear Faraday rotation for a sample of cold atoms both with cw and modulated laser beams. The use of retroreflected beam alleviated the problem of mechanical perturbation of the cold atoms by the probe beam. In contrast to previous experiments with pure quantum states of oriented spins, the NFR measurements allow control and convenient studies of long-lived superposition states of aligned spins, i.e. quantum superpositions of Zeeman sublevels belonging to a given  $F$ . In particular, we are able to vary the degree of Zeeman coherence and monitor its build-up and decay, both in the stationary regime ( $B \simeq 0$ ), and for the Larmor frequencies up to 10 MHz. In addition to its potential for QSE, the NFR effect can be used for measuring a wide range of transient and static magnetic fields with 10  $\mu$ s time resolution, sub-mG sensitivity, and mm spatial resolution given by the size of the cold atom cloud or the beam waist size. The current results are limited mostly by finite lifetime of trapped atoms and power broadening by the probe beam. Transfer of atoms into an optical dipole trap would make probing time much longer ( $\sim 1$  s) and the light-atom coupling more effective whereas the use of separate pump and probe beams as

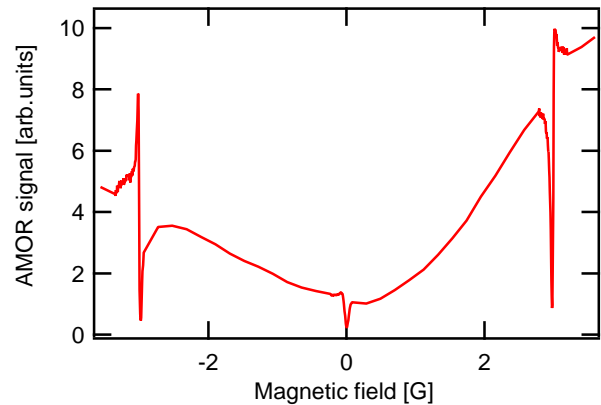


FIG. 6: NFR with amplitude modulated light (AMOR). The narrow central resonance is a typical NFR zero-field resonance and the two high field resonances at  $\pm 3$  G result from amplitude modulation of the light with  $\Omega_m = 2.8$  MHz. Presence of such high-field resonances allows for precision magnetometry of non-zero magnetic fields. The broad background is the LFR. The slight asymmetry of resonance shapes can be attributed to experimental setup imperfection.

opposed to a single pump-probe beam would alleviate power broadening limitations.

The authors would like to acknowledge valuable discussions with D. Budker, W. Chalupczak, R. Kaiser, M. Kubasik and S. Pustelny. This work has been supported by the Polish Ministry of Science (grant # N N505 092033 and N N202 046337) and NSF Global Scientists Program.

- 
- [1] S. Franke-Arnold, M. Arndt, and A. Zeilinger, J. Phys. B **34**, 2527 (2001).
  - [2] G. Labeyrie, C. Miniatura, and R. Kaiser, Phys. Rev. A **64**, 033402 (2001).
  - [3] J. Nash and F. A. Narducci, Journ. Mod. Optics **50**, 2667 (2003).
  - [4] M. L. Terraciano, M. Bashkansky, and F. K. Fatemi, Phys. Rev. A **77**, 063417 (2008).
  - [5] E. Arimondo, in *Progress in Optics*, edited by E. Wolf (Elsevier, Amsterdam, 1996), vol. 35, pp. 259–354.
  - [6] M. Fleischhauer, A. Imamoglu, and J. P. Marangos, Rev. Mod. Phys. **77**, 633 (2005).
  - [7] D. Budker, W. Gawlik, D. F. Kimball, S. M. Rochester, V. V. Yashchuk, and A. Weis, Rev. Mod. Phys. **74**, 1153+ (2002).
  - [8] R. Drampyan, S. Pustelny, and W. Gawlik, Phys. Rev. A **80**, 033815 (2009).
  - [9] B. Julsgaard, J. Sherson, J. L. Sørensen, and E. S. Polzik, J. Opt. B **6**, 5 (2004).
  - [10] T. Isayama, Y. Takahashi, N. Tanaka, K. Toyoda, K. Ishikawa, and T. Yabuzaki, Phys. Rev. A **59**, 4836 (1999).
  - [11] S. Wildermuth, S. Hofferberth, I. Lesanovsky, S. Groth,

- P. Krüger, J. Schmiedmayer, and I. Bar-Joseph, Appl. Phys. Lett. **88**, 264103 (2006).
- [12] M. Vengalattore, J. M. Higbie, S. R. Leslie, J. Guzman, L. E. Sadler, and D. M. Stamper-Kurn, Phys. Rev. Lett. **98**, 200801 (2007).
- [13] M. L. Terraciano, M. Bashkansky, and F. K. Fatemi, Opt. Express **16**, 13062 (2008).
- [14] G. W. Series, Proc. Phys. Soc. **88**, 995 (1966).
- [15] C. Cohen-Tannoudji and F. Laloë, J. Phys. (Paris) **28**, 505, 722 (1967).
- [16] M. Kubasik, M. Koschorreck, M. Napolitano, S. R. de Echaniz, H. Crepaz, J. Eschner, E. S. Polzik, and M. W. Mitchell, Phys. Rev. A **79**, 043815 (2009).
- [17] D. Budker, D. F. Kimball, V. V. Yashchuk, and M. Zolotarev, Phys. Rev. A **65**, 055403 (2002).
- [18] W. Gawlik, L. Krzemieñ, S. Pustelny, D. Sangla, J. Zachorowski, M. Graf, A. O. Sushkov, and D. Budker, Appl. Phys. Lett. **88**, 131108 (2006).